Biomimetic surface modifications of stainless steel targeting dairy fouling mitigation and bacterial adhesion

Sawsen Zouaghi, Séverine Bellayer, V. Thomy, Thomas Dargent, Yannick Coffinier, Christophe Andre, Guillaume Delaplace, Maude Jimenez

BIOMIMETIC SURFACE MODIFICATIONS OF STAINLESS STEEL TARGETING DAIRY FOULING MITIGATION AND BACTERIAL ADHESION

Sawsen ZOUAGHI[1], Séverine BELLAYER[1], Vincent THOMY[2], Thomas DARGENT[2], Yannick COFFINIER[2], Christophe ANDRE[1,3], Guillaume DELAPLACE[1], Maude JIMENEZ[1]*

[1]*Université de Lille, Unité Matériaux et Transformations (UMET), UMR 8207, F-59000 Lille, France.*

[2] *Institut d'Electronique, de Microélectronique et de Nanotechnologie (IEMN), UMR 8520, F-59000 Lille, France.*

[3] *Hautes Etudes d'Ingénieur (HEI), rue de Toul, F-59000 Lille, France.*

*corresponding author: maude.jimenez@univ-lille1.fr

ABSTRACT

This work aims at presenting and comparing the antifouling and antibacterial behaviour of three biomimetic surfaces targeting dairy fouling reduction, namely atmospheric plasma-sprayed silane-based thin films, lubricated slippery surfaces and femtosecond laser textured lotus-like surfaces. Fouling tests were conducted on a pilot-scale pasteurization plant fed with a model whey protein and calcium foulant solution and tested samples were placed in isothermal holding-like conditions. Detailed characterizations of the substrates before and after fouling test allowed connecting their surface properties to their antifouling performances. The best result was obtained with the nano-rough plasma coatings which led to a substantial fouling reduction for two consecutive pasteurisation runs. These surfaces were subsequently tested towards bacterial adhesion with three different foodborne pathogenic strains, again demonstrating better performances than bare stainless steel.

KEYWORDS

Antifouling, dairy, biomimetism, antibacterial, plasma, slippery liquid-infused surface

SYMBOLS

θ	Contact angle (°)	
γ	Surface energy (mN/m)	
Δm	difference between sample mass before and after the fouling test (mg)	
F%	Fouling grade (-)	
Superscripts:	D	dispersive
	P	polar
	T	total
Subscripts:	S	Solid
	L	Liquid
	V	Vapour

INTRODUCTION

Fouling is an ongoing issue in dairy industries, where thermal treatments are essential to ensure food safety and to extend the products' shelf-life (Boxler et al., 2013; Rosmaninho et al., 2007). The heat-induced accumulation of proteins and minerals on the equipment walls indeed impairs the proper execution of thermal treatments and burdens the processes' cost and environmental impact through production loss as well as important water and chemical use during the clean-in-place procedures. Fouling control could then allow moving towards less expensive and more eco-responsible processes. Tuning the surface properties of stainless steel is one possible pathway to mitigate fouling, as it would impact the interactions at the substrate/fluid interface (Barish and Goddard, 2013; Santos et al., 2004). The most classical approach for dairy fouling management consists in minimizing surface energy (especially polar components) and surface roughness (Boxler et al., 2013; Gordon et al., 1968; Santos et al., 2004). However, numerous other pathways can be followed to achieve fouling mitigation, like hydrophilic polymer brushes, hydrogels, zwitterionic coatings (Mérian and Goddard, 2012) or bio-inspired surfaces.

Indeed, the remarkable surface properties of several living organisms recently drew the attention of the scientific community toward biomimetic approaches for the design of new functional surfaces, intended to solve issues such as fouling. The most well-known example of biomimetic surface engineering is the superhydrophobic lotus-like surface which presents self-cleaning abilities in certain conditions, due to its particular wetting regime (Yan et al., 2011). Numerous papers indeed report different methods to design synthetic superhydrophobic surfaces through cutting-edge technologies, such as structure growth (Coffinier et al., 2007; Nguyen et al., 2014; Verplanck et al., 2007), lithography (Bixler et al., 2014) often coupled with dry or wet etching, vacuum plasma treatments (Jung and Bhushan, 2009), layer-by-layer deposition (Bravo et al., 2007), sol-gel processes (Mahltig and Böttcher,

2003; Yu et al., 2007) or electro-spinning/-spraying (Ding et al., 2008). Aside from the overly famous lotus-like surface, the tunable wettability of gecko toes (Liu et al., 2012) as well as the segregated hydrophilicity/hydrophobicity of *Salvinia* leaves (Barthlott et al., 2010) are also worth to be reported, as they have also been studied and mimicked to design functional surfaces. Overall, biomimicry offers multiple possibilities that could be integrated in research strategies aiming at fouling management.

Therefore, the purpose of this work is to present and to compare the behaviours of different biomimetic surfaces (namely atmospheric plasma-sprayed silane-based thin films, lubricated slippery surfaces and femtosecond laser textured lotus-like surfaces) when exposed to isothermal dairy fouling and to bacterial suspensions, in order to assess the potential of such bio-inspired substrates for food-related fouling management applications.

EXPERIMENTAL DETAILS

1.1.Biomimetic surfaces preparation

Figure 1 presents schematic representations of the three studied biomimetic surfaces and the experimental details for their design are detailed hereafter.

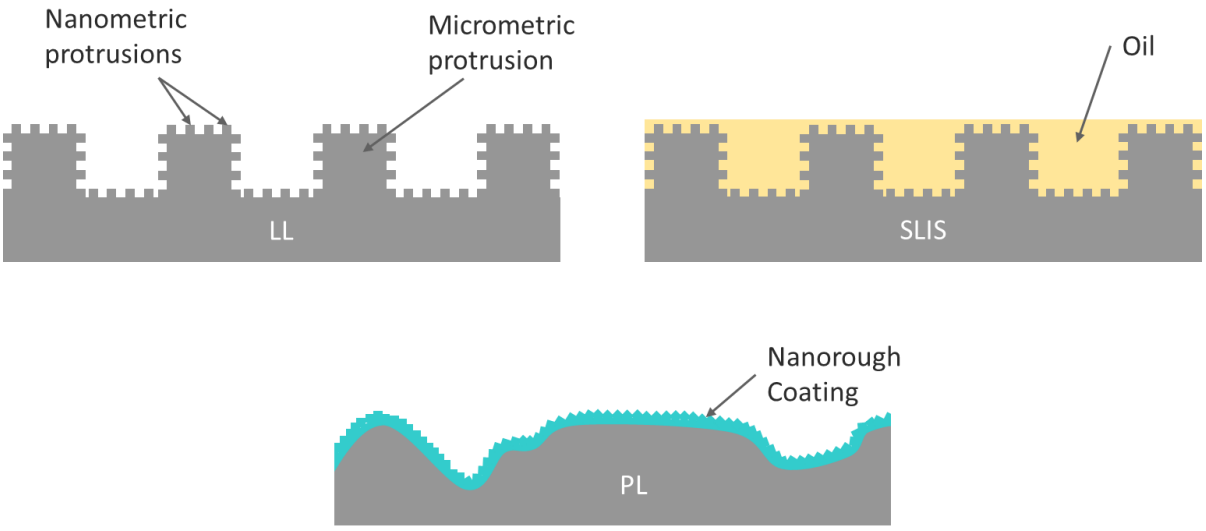

Figure 1. Schematic representation of the three biomimetic surfaces: laser ablated Lotus-like surface (LL), slippery liquid-infused surface (SLIS) and nano-rough plasma coated surface (PL).

1.1.1. Reference surfaces

The control surfaces used in this work were 316L 2B stainless steel (SS) coupons (16 x 45 x 1 mm^3) from Sapim Inox (France). They were first degreased in a 50/50 (v/v) ethanol/acetone mixture and washed in a 2% RBS detergent (Sigma-Aldrich) solution at 65 °C. They were then rinsed twice in hot deionised water, twice in room temperature (RT) water and dried at RT.

1.1.2. Lotus-like surfaces

In order to design lotus-like surfaces (LL), stainless steel surfaces were textured via femtosecond laser ablation as described by Moradi et al. (2016, 2015) in order to generate hierarchical micro- and nanostructures. They were then cleaned by ozonolysis (UV/ozone cleaner) and directly silanized in a 10^{-3} M solution of (1*H*, 1*H*, 2*H*, 2*H*-perfluorodecyl)

trichlorosilane (Sigma Aldrich) in n-hexane for 4 hours at RT. The textured silanized surfaces were then rinsed under hexane and dichloromethane flow and dried under nitrogen stream.

1.1.3. Slippery liquid infused surfaces

Biomimetic slippery liquid-infused surfaces (SLIS), inspired from *Nepenthes* pitcher plants (Wong et al., 2011) were designed, as described by Zouaghi et al. (2017), by impregnating the lotus-like surfaces with Krytox 103 GPL (DuPont), a perfluorinated oil chosen for its chemical inertness and low surface tension (20 mN/m). The oil was poured dropwise on the surfaces, which were then left tilted for 15 min to remove the excess oil and stored away from dust until tested. The purpose for surface texturing prior to impregnation was to enhance the retention of oil on the substrate, through capillarity.

1.1.4. Nano-rough plasma coatings

Plasma-sprayed coatings (PL) were obtained as described by Zouaghi et al. (2018a), by spraying a silicon-containing precursor (hexamethyldisiloxane, HMDSO, Sigma Aldrich) at 35 g/h in the afterglow of an alternative current discharge in pure nitrogen. The plasma source and the precursor spraying device were mounted on a 3-axis automaton, allowing scanning them at 3 cm over the substrate. To enhance coating adhesion, an activation step consisting in 4 passes of nitrogen plasma without precursor spraying was performed before coating. Before testing, the samples were aged for a week in air and away from dust.

1.2.Surface characterisations

Water contact angles (WCA) of the different surfaces were measured on a DSA100 drop shape analyser (Krüss, Germany) with 2 µL droplets (Equation 1, (Adamson and Gast, 1967)). Surface free energies (SFE) were calculated from the contact angles of pure deionised water, formamide and diiodomethane (purity ≥ 99%, Sigma Aldrich) following the OWRK method (Equation 2) (Owens and Wendt, 1969). To assess their full wettability profile,

contact angle hysteresis (CAH) of the biomimetic surfaces were calculated *via* the tilting method. Data are representative of three different measurements on three droplets deposed randomly on the surfaces.

$$\cos(\theta) = \frac{\gamma_{SV} - \gamma_{SL}}{\gamma_{LV}} \quad \textbf{Equation 1}$$

$$\gamma_{SL} = \gamma_S + \gamma_L - 2\left(\sqrt{\gamma_S^D \cdot \gamma_L^D} + \sqrt{\gamma_S^P \cdot \gamma_L^P}\right) \quad \textbf{Equation 2}$$

Arithmetic mean roughness (Ra) of the samples was measured with a KLA Tencor contract profilometer. The scanning speed was 20 µm/s and scan length was 500 µm. Results are representative of three measurements on three different scans.

Scanning electron microscopy (SEM) pictures of the samples were taken on a Hitachi S4700 device at 5 kV, 15 µA.

1.3.Fouling test

The procedures for fouling tests has been detailed in previous works (Zouaghi et al., 2018, 2017a). Briefly, fouling tests were carried out with a model foulant fluid (MFF) to ensure repeatability. The MFF was a 1% whey protein concentrate solution (Promilk FB852, Ingredia) in reverse osmosis water. The calcium concentration was adjusted to 100 ppm by $CaCl_2$ addition. Five hundred litres of this MFF were freshly prepared for each test. The pilot-scale pasteurisation unit was composed of a stirred storage tank connected to two consecutive plate heat exchangers (PHE) where the MFF was circulated at 300 L/h counter-current to hot water. The first PHE pre-heated the fluid up to 60°C and the second PHE heated the fluid up to 85°C (pasteurisation temperature). Sample-holders were connected at the outlet of the heating section of the installation, so that modified and control surfaces were exposed to the hot dairy fluid without being heated, in the same conditions as inside a holding section. MFF was circulated for 1.5 h at the flow 300 L/h and then a 20 min water rinse (300 L/h) was performed. The purpose of simple water rinses was to screen surfaces that could allow for the

softening of cleaning conditions. Samples were then taken out of the sample holders, left to dry for at least two days in a ventilated cold room before any further analysis, or, if they were free of fouling, submitted to additional fouling and rinsing tests.

In order to easily describe their fouling behaviour, a fouling grade, "F%", was calculated for each surface after the final fouling test, according to Equation 3, where Δm represents the difference between sample mass before and after the fouling test.

$$F\% = \frac{\Delta m_x - \Delta m_{Ref}}{\Delta m_{Ref}} \times 100 \qquad \textbf{Equation 3}$$

Results are representative of 3 fouling tests performed on different days, each involving at least 3 replicates for each surface.

1.4.Static bacterial adhesion test

It is of great importance for food-contacting materials to be evaluated towards bacterial adhesion, to prevent both microbiological growth in the equipment and contamination of the products. Therefore, bacterial adhesion tests were carried out on the biomimetic surface with the best antifouling performances. Three bacterial strains, namely *Staphylococcus aureus* CIP 4.83 (CRBIP, France), *Salmonella enterica* CIP 8297 (CRBIP, France) and *Listeria monocytogenes* ATCC 35152 (LM/NCTC, United Kingdom) were chosen for their relevance regarding the considered field of study, *i.e*. dairy pasteurisation, and for their shape (rod and round) as well as Gram-staining diversity.

For all strains, pre-cultures were prepared by inoculating 5 mL of tryptic soy broth (TSB) with 100 µL from the preservation tubes. They were then incubated at 37°C (optimal growth temperature for mesophilic bacteria) for 24h. Main cultures were obtained by inoculating 50 mL of TSB with 100 µl of pre-culture. They were stopped in the late exponential phases and cells were harvested and washed twice with physiological water (0.9% NaCl solution in sterile ultrapure water). Cell concentrations of the final suspensions were checked through

absorbance measurements at 620 nm and the appropriate dilutions to obtain 10^7 colony-forming units (CFU) per mL were performed.

Substrates were then covered with 3 ml of those bacterial suspensions and left in static conditions for 1 h. After rinsing with physiological water under low stirring (shaker plate, 60 rpm), the adhered cells were stained with acridine orange and counted *via* fluorescence microscopy (Olympus BX43).

The choice of these mild test conditions ((hydrodynamics and temperature) was made in order to characterise the adhesion of unharmed strains on the modified surfaces and assess their potential application in a food-related context.

RESULTS AND DISCUSSIONS

1.5.Clean surfaces characterizations

Table 1 gathers wettability, surface energy (divided between the dispersive (γ^D) and the polar (γ^P) components, roughness and adhesion features for all the studied samples. All surface treatments altered the wettability of the original stainless steel (SS) surface.

Table 1. Water contact angle, surface energy, OWRK correlation coefficient, roughness and adhesion rates of the different surfaces.

Sample	WCA (°)	Surface free energy (mN/m)			OWRK Coef.	Ra (µm)
		γ^{Total}	γ^D	γ^P		
Stainless steel (SS)	84.2 ± 2.6	41.9 ± 4.3	38.2 ± 0.9	3.7 ± 2.5	0.97	0.07 ± 0.01
Plasma coating (PL)	94.3 ± 2.2	41.5 ± 4.7	34.3 ± 2.3	7.1 ± 2.5	0.98	0.05 ± 3.10^{-3}
Slippery liquid-infused surface (SLIS)	111.6 ± 1.3	18.1 ± 3.2	16.2 ± 2.2	1.9 ± 0.9	0.97	-
Lotus-like surface (LL)	132.9 ± 1.6	-	-	-	-	36.0 ± 2.0

Plasma spraying increased the WCA from 84.2 ± 2.6° to 94.3 ± 2.2° due to the hydrophobicity and low surface tension of the plasma coating precursor (HMDSO). Expectedly, LL surface modification triggered a considerable increase of Ra (to 36.0 ± 2.0

µm) and of WCA, reaching 132.9 ± 1.6°. Moreover, dynamic goniometry measurements allowed to establish that LL surfaces presented very low CAH (2.6 ± 0.8°). The association of hierarchical roughness (Figure 2B) to low surface energy from the silanisation is indeed known to yield high contact angles due to the establishment of the suspended Cassie-Baxter's wetting regime. This regime is characterised by the presence of air between the solid substrate and the fluid (Lafuma and Quéré, 2003), hence leading to low adhesion of fluid to the substrate, which translates into low CAH values, as it is the case here.

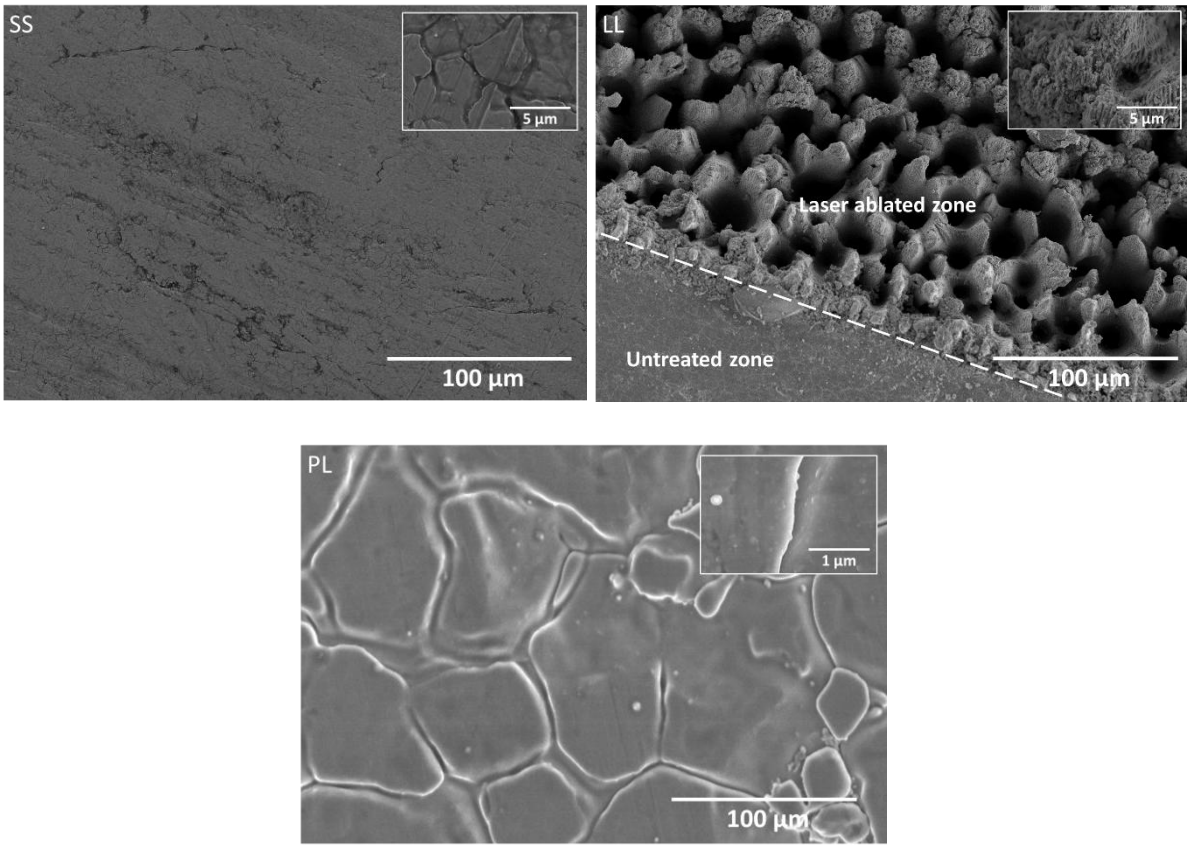

Figure 2. SEM micrographs of bare stainless steel (SS), laser ablated Lotus-like stainless steel (LL) and plasma coated stainless steel (PL).

SFE values for LL surfaces could not be calculated based on contact angle measurements as it was done for the other substrates. Indeed, the morphology of such surfaces strongly impacts the shape of deposed droplet, whose contact angle cannot be accurately used to calculate surface energy values.

For SS, PL and SLIS surfaces, all OWRK correlation coefficients are above 0.90, indicating that the surfaces fit the chosen surface energy calculation model. Overall, SFE, measured at 41.9 ± 4.3 mN/m for native SS, was also impacted by surface modifications. Expectedly, SLIS exhibited the lowest surface energy (18.1 ± 3.2 mN/m). Subdivision of the total SFE (γ^{Total}) into dispersive (γ^{D}) and polar (γ^{P}) components further highlighted the remarkably low γ^{P} of SLIS surface (1.9 ± 0.9 mN/m). This SFE value, associated with the menisci visible on both sides of the water droplet (Figure 3) and to their remarkably low CAH (0.6 ± 1.9°), attests that the SLIS surface is completely covered with an oil film, with no emerged protrusion (Smith et al., 2013).

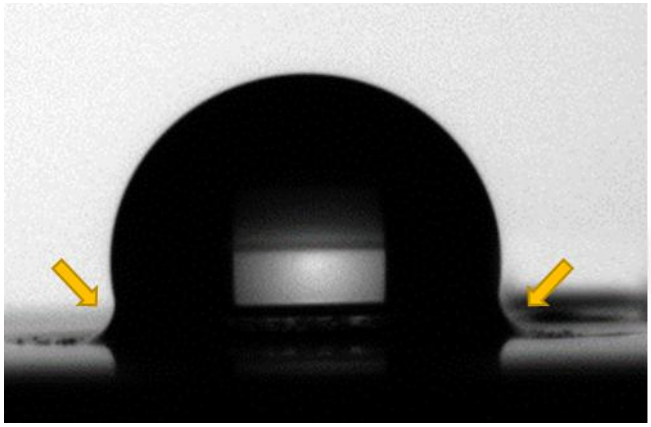

Figure 3. A 2 µL water droplet on a SLIS surface, presenting two menisci at its basis.

It is interesting to notice that, in the case of PL surfaces, the increase in WCA is not associated with an SFE decrease. Indeed, the SFEs of SS and PL, 41.9 ± 4.3 mN/m and 41.5 ± 4.7 mN/m respectively, are very similar. However, the difference between their polar components (γ^{P}) is noticeable. Considering that γ^{P} of the PL coating is superior to that of bare stainless steel, a lower WCA should be expected for this surface compared to SS. Goniometry measures proved the contrary, with 94.3 ± 2.2° for PL versus 84.2 ± 2.6° for SS. As surface morphology is known to influence apparent contact angles (Wenzel wettability model, (Wenzel, 1949)), it is likely that a change in surface morphology played a role in the establishment of this high WCA value. Profilometry measurements in fact indicate a slight

change in surface roughness after plasma coating (from 0.07 ± 0.01 to 0.05 ± 3.10^{-3}). Furthermore, SEM and AFM analyses (Figure 2 and Figure 4) showed that PL coatings present a pronounced nano-roughness, in accordance with previous findings (Zouaghi et al., 2018).

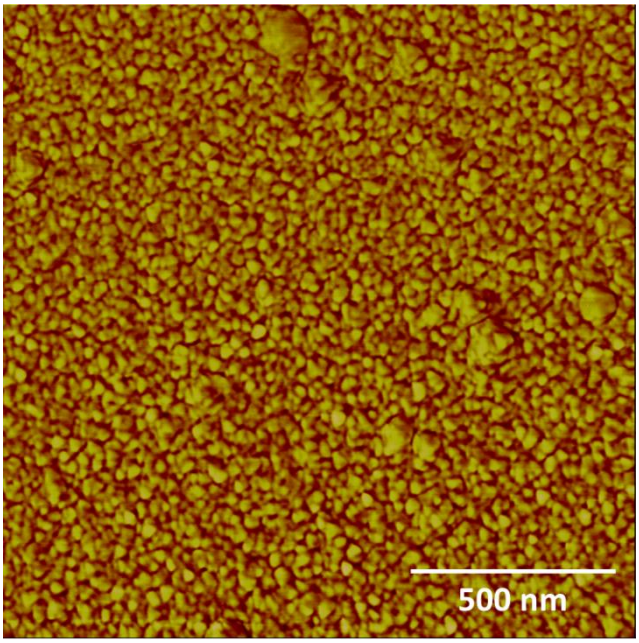

Figure 4. AFM imaging of the plasma coating (PL) surface.

1.6.Fouling behaviours

All surfaces were submitted to several consecutive fouling tests (pasteurisation and rinsing), and the results are presented in Table 2. The durability is defined in this study by the number of cycles through which a surface maintains its initial antifouling performance.

At first glance, it is obvious that all surfaces achieved very different antifouling performances. Lotus-like surfaces (LL) presented very poor results, as they exhibited more deposit than bare stainless steel. On the other hand, PL and SLIS surfaces showed good antifouling performances, as PL allowed a reduction of fouling density by 99.5 ± 9.5 % and no trace of deposit was found on SLIS surfaces.

Table 2. Fouling performance and durability of the different surfaces.

Sample	Fouling Density (mg/cm²)	F%	WCA after fouling tests	Durability (cycles)
Stainless steel (SS)	30.8 ± 4.0	Control	-	-
Plasma coating (PL)	2.1 ± 0.2	-93.2	67.3 ± 4.2	2
Slippery liquid-infused surfaces (SLIS)	0.0 ± 0.0	-100	139.1 ± 3.5	1
Lotus-like surface (LL)	57.4 ± 14.3	+ 86.4	-	-

This difference in fouling performance is most certainly mainly driven by the differences in surface morphology. Indeed, while the best performance was achieved by SLIS, which presents a smooth, liquid interface, the worst one was that of the rougher surface, *i.e.* LL (Ra of 36µm). It was indeed demonstrated that the open morphology and deep relief of LL surfaces favours deposit growth during the pasteurisation run, due to interlocking phenomena between the substrate and the fouling agents at the interface (Zouaghi et al., 2017b), that is to say that fouling agents were able to penetrate the substrate, creating a very strong anchoring for further build-up (Brady and Singer, 2000). Plasma coatings (PL) exhibited satisfactory performances, as they allowed reducing fouling by more than 90%. Those good results are attributed to the conjugated effect of surface chemistry, *i.e.* siloxane from the HMDSO precursor, and surface morphology, *i.e.* nano-roughness (Zouaghi et al., 2018).

Durability was also very different depending on surface type. Bare SS and LL surfaces could not be re-used after rinsing, due to the important presence of dairy deposits. The plasma coatings managed to prevent fouling through two consecutive fouling cycles. Past this threshold, fouling performances were close to those of bare SS and the antifouling properties could not be recovered. A possible explanation is that a thin layer of protein remains from the previous cycle, causing the WCA decrease and acting as an anchor that promotes deposit growth. This hypothesis seems to be corroborated by the change in WCA witnessed after the

fouling test (Table 2: 67.3° vs 94.3°), which can be due to the presence of hydrophilic protein on the surface.

On the other hand, highly slippery SLIS surfaces only kept their properties through one fouling test. The very high WCA observed after fouling test (139.1°) points toward oil depletion caused by the exposure to tangential flow. Emerged solid micro- and nanostructures have indeed been shown to cause this apparent hyperhydrophobicity (Zouaghi et al., 2017b).

At this point, it can be admitted that PL surfaces can be considered as superior to the other two biomimetic surfaces for fouling mitigation, as they present good antifouling properties and the best durability. Indeed, LL surfaces presented poor fouling performances and SLIS surfaces poor durability. Thus, bacterial adhesion tests were carried out only on PL surfaces, in order to establish their ability to prevent bacterial adhesion.

1.7.Bacterial adhesion test

Figure 5 presents the results from the adhesion tests carried out on SS and PL surfaces with *S. aureus*, *L. monocytogenes* and *S. enterica*.

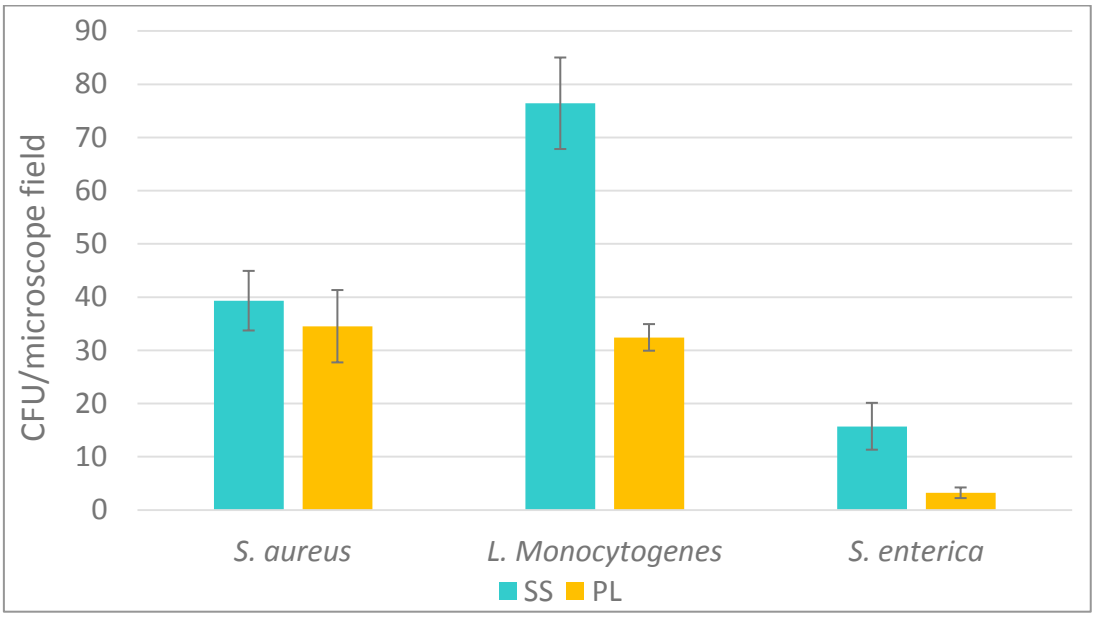

Figure 5. Adhesion rates (CFU/microscope field) for *S. aureus*, *L. Monocytogenes* and *S. enterica* on bare stainless steel and plasma coating.

For all the strains, adhesion levels were smaller on the plasma coating than on the bare SS reference, although the difference is much more striking for the two rod-shaped bacteria (*L. monocytogenes and S. enterica*). Indeed, for those two strains, plasma coating allowed to reduce the number of adhered CFU by 58% and 80% respectively. In the case of S. aureus, a difference is also observed but it does not exceed the error margins. This is probably due to the fact that S. aureus is a round-shaped bacterium and that this geometry allows it to easily penetrate into the grain boundaries of the coated surface. Indeed, the coating thickness does not permit it to fill in the grain boundaries of the SS substrate (Zouaghi et al., 2018). Figure 6 indeed reveals that a significant number of adhered S. aureus cells are located into the grain boundaries of the surface, highlighting the importance of roughness and surface morphology in the control of bacterial adhesion.

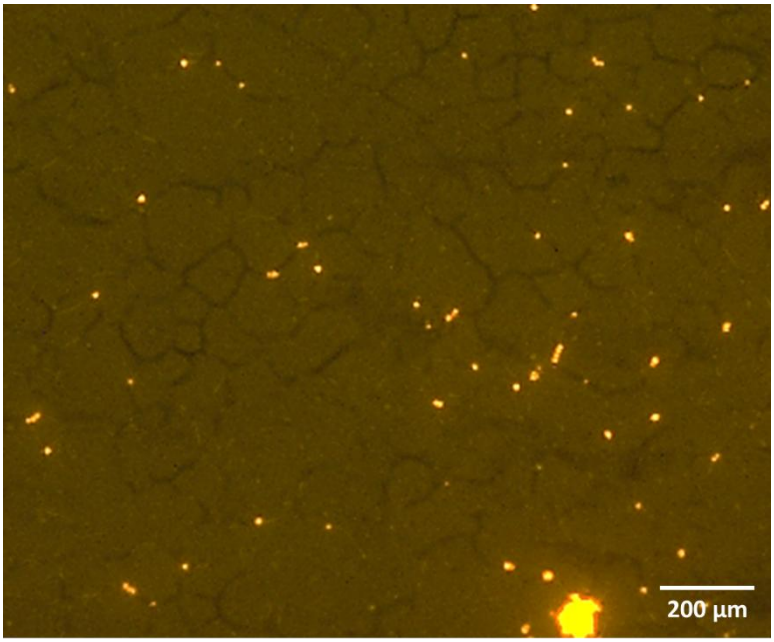

Figure 6. Fluorescence microscopy picture of *S. aureus* on a PL surface. A significant amount of cells are located in the grain boundaries of the surface.

CONCLUSIONS

This work presented the performances of three bio-inspired surfaces regarding dairy fouling and foodborne pathogenic bacteria adhesion. It was shown that the biomimetic approach, was very promising, although further research is needed to progress towards large-scale manufacture and industrialisation of such surfaces. Indeed, out of the three described surfaces, two, namely slippery liquid infused surfaces and nano-rough plasma coatings, exhibited significant fouling reduction compared to the reference (bare stainless steel). The isothermal pilot fouling tests therefore allowed to screen and select the surfaces which should be tested as heat-transfer surfaces in further research.

Static bacterial adhesion tests showed that plasma coatings showed a beneficial effect for the limitation of adhesion of unharmed bacterial strains, highlighting their potential in food-related applications.

The impact of surface morphology on both dairy fouling and micro-organism adhesion was also highlighted, as very rough lotus-like surfaces showed increased fouling amounts compared to bare stainless steel, due to the wetting mode transition which was triggered by the environmental conditions inside the pilot pasteuriser, while the smooth liquid surface of slippery surfaces presented excellent antifouling properties.

Although the economic features of the biomimetic surfaces are not assessed yet at this stage of their development, their implementation in thermal treatments equipment could undoubtedly lead to significant savings, from both financial and environmental points of view, through the softening of cleaning-in-place procedures. This pathway should thus be pursued in order to optimize the durability and the food compatibility of the surfaces. For instance, the slippery surfaces could benefit from the optimisation of their morphology to enhance oil retention, for example by using electrochemical etching to obtain porous stainless steel (Lee et al., 2015), and from the investigation of alternative lubricants, more suited to a

food-related application. On the other hand, the durability of plasma coatings could be improved through the tuning of their manufacturing parameters, using for example experimental design to adjust precursor flow rate, nozzle-to-substrate distance or whether scanning speed.

ACKNOWLEDGEMENTS

The authors gratefully acknowledge the University of Lille and the Hauts-de-France Region for funding the PhD scholarship and the French National Agency (ANR) for its financial support (ECONOMICS project (ANR-17-CE08-0032)). They also thank the Common Microscopy Centre of Lille University for the access to equipment.

REFERENCES

Adamson, A.W., Gast, A.P., 1967. Physical chemistry of surfaces, Wiley. ed. Interscience publishers New York.

Barish, J.A., Goddard, J.M., 2013. Anti-fouling Surface Modified Stainless Steel for Food Processing. Food Bioprod. Process. 91, 352–361. https://doi.org/http://dx.doi.org/10.1016/j.fbp.2013.01.003

Barthlott, W., Schimmel, T., Wiersch, S., Koch, K., Brede, M., Barczewski, M., Walheim, S., Weis, A., Kaltenmaier, A., Leder, A., Bohn, H.F., 2010. The Salvinia Paradox: Superhydrophobic Surfaces with Hydrophilic Pins for Air Retention Under Water. Adv. Mater. 22, 2325–2328.

Bixler, G.D., Theiss, A., Bhushan, B., Lee, S.C., 2014. Anti-Fouling Properties of Microstructured Surfaces Bio-Inspired by Rice Leaves and Butterfly Wings. J. Colloid an interface Sci. 419, 114–133. https://doi.org/http://dx.doi.org/10.1016/j.jcis.2013.12.019

Boxler, C., Augustin, W., Scholl, S., 2013. Fouling of Milk Components on DLC Coated Surfaces at Pasteurization and UHT Temperatures. Food Bioprod. Process. 91, 336–347. https://doi.org/http://dx.doi.org/10.1016/j.fbp.2012.11.012

Brady, R.F., Singer, I.L., 2000. Mechanical Factors Favoring Release from Fouling Release Coatings. Biofouling 15, 73–81.

Bravo, J., Zhai, L., Wu, Z., Cohen, R.E., Rubner, M.F., 2007. Transparent superhydrophobic films based on silica nanoparticles. Langmuir 23, 7293–7298.

Coffinier, Y., Janel, S., Addad, A., Blossey, R., Gengembre, L., Payen, E., Boukherroub, R., 2007. Preparation of superhydrophobic silicon oxide nanowire surfaces. Langmuir 23, 1608–1611.

Ding, B., Ogawa, T., Kim, J., Fujimoto, K., Shiratori, S., 2008. Fabrication of a super-hydrophobic nanofibrous zinc oxide film surface by electrospinning. Thin Solid Films 516, 2495–2501.

Gordon, K.P., Hankinson, D.J., Carver, C.E., 1968. Deposition of Milk Solids on Heated Surfaces1. J. Dairy Sci. 51, 520–526.

Jung, Y.C., Bhushan, B., 2009. Mechanically Durable Carbon Nanotube−Composite Hierarchical Structures with Superhydrophobicity, Self-Cleaning, and Low-Drag. ACS Nano 3, 4155–4163. https://doi.org/10.1021/nn901509r

Lafuma, A., Quéré, D., 2003. Superhydrophobic States. Nat. Mater. 2, 457–460.

Lee, C., Kim, A., Kim, J., 2015. Electrochemically Etched Porous Stainless Steel for Enhanced Oil Retention. Surf. Coat. Technol. 264, 127–131.

Liu, K., Du, J., Wu, J., Jiang, L., 2012. Superhydrophobic gecko feet with high adhesive forces towards water and their bio-inspired materials. Nanoscale 4, 768–772.

Mahltig, B., Böttcher, H., 2003. Modified silica sol coatings for water-repellent textiles. J. sol-gel Sci. Technol. 27, 43–52.

Mérian, T., Goddard, J.M., 2012. Advances in Nonfouling Materials: Perspectives for the Food Industry. J. Agric. Food Chem. 60, 2657–2943.

Moradi, S., Hadjesfandiari, N., Toosi, S.F., Kizhakkedathu, J.N., Hatzikiriakos, S.G., 2016. Effect of Extreme Wettability on Platelet Adhesion on Metallic Implants: From Superhydrophilicity to Superhydrophobicity. ACS Appl. Mater. Interfaces 8, 17631–17641. https://doi.org/10.1021/acsami.6b03644

Moradi, S., Kamal, S., Hatzikiriakos, S.G., 2015. Superhydrophobic Laser-Ablated Stainless Steel Substrates Exhibiting Cassie-Baxter Stable State. Surf. Innov. 3, 151–163.

Nguyen, T.P.N., Boukherroub, R., Thomy, V., Coffinier, Y., 2014. Micro-and nanostructured silicon-based superomniphobic surfaces. J. Colloid Interface Sci. 416, 280–288.

Owens, D.K., Wendt, R.C., 1969. Estimation of the surface free energy of polymers. J. Appl. Polym. Sci. 13, 1741–1747. https://doi.org/10.1002/app.1969.070130815

Rosmaninho, R., Santos, O., Nylander, T., Paulsson, M., Beuf, M., Benezech, T., Yiantsios, S., Andritsos, N., Karabelas, A., Rizzo, G., Muller-Steinhagen, H., Melo, L.F., 2007. Modified Stainless Steel Surfaces Targeted to Reduce Fouling - Evaluation of Fouling by Milk Components. J. Food Eng. 80, 1176–1187. https://doi.org/http://dx.doi.org/10.1016/j.jfoodeng.2006.09.008

Santos, O., Nylander, T., Rosmaninho, R., Rizzo, G., Yiantsios, S., Andritsos, N., Karabelas, A., Muller-Steinhagen, H., Melo, L., Boulange-Petermann, L., Gabet, C., Braem, A., Tragardh, C., Paulsson, M., 2004. Modified Stainless Steel Surfaces Targeted to Reduce Fouling - Surface Characterization. J. Food Eng. 64, 63–79. https://doi.org/http://dx.doi.org/10.1016/j.jfoodeng.2003.09.013

Smith, J.D., Dhiman, R., Anand, S., Reza-Garduno, E., Cohen, R.E., McKinley, G.H., Varanasi, K.K., 2013. Droplet Mobility on Lubricant-Imprengated Surfaces. Soft Matter 9, 1772–1780.

Verplanck, N., Galopin, E., Camart, J.-C., Thomy, V., 2007. Reversible Electrowetting on Superhydrophobic Silicon Nanowires. Nano Lett. 7, 813–817.

Wenzel, R.N., 1949. Surface roughness and contact angle. J. Phys. Chem. 53, 1466–1467.

Wong, T.S., Kang, S.H., Tang, S.K., Smythe, E.J., Hatton, B.D., Grinthal, A., Aizenberg, J., 2011. Bioinspired Self-Repairing Slippery Surfaces with Pressure-stable Omniphobicity. Nature 7365, 443–447.

Yan, Y.Y., Gao, N., Barthlott, W., 2011. Mimicking Natural Superhydrophobic Surfaces and

Grasping the Wetting Process: A Review on Recent Progress in Preparing Superhydrophobic Surfaces. Adv. Colloid Interface Sci. 169, 80–105. https://doi.org/http://dx.doi.org/10.1016/j.cis.2011.08.005

Yu, M., Gu, G., Meng, W.-D., Qing, F.-L., 2007. Superhydrophobic cotton fabric coating based on a complex layer of silica nanoparticles and perfluorooctylated quaternary ammonium silane coupling agent. Appl. Surf. Sci. 253, 3669–3673.

Zouaghi, S., Six, T., Bellayer, S., Coffinier, Y., Abdallah, M., Chihib, N.-E., André, C., Delaplace, G., Jimenez, M., 2018. Atmospheric pressure plasma spraying of silane-based coatings targeting whey protein fouling and bacterial adhesion management. Appl. Surf. Sci. 455, 392–402. https://doi.org/https://doi.org/10.1016/j.apsusc.2018.06.006

Zouaghi, S., Six, T., Bellayer, S., Moradi, S., Hatzikiriakos, S., Dargent, T., Thomy, V., Coffinier, Y., Andre, C., Delaplace, G., 2017a. Biomimetic nanostructured surfaces for antifouling in dairy processing. S6-Microfluidique, nanofluidique écoulements à interface.

Zouaghi, S., Six, T., Bellayer, S., Moradi, S., Hatzikiriakos, S.G., Dargent, T., Thomy, V., Coffinier, Y., André, C., Delaplace, G., Jimenez, M., 2017b. Antifouling Biomimetic Liquid-Infused Stainless Steel: Application to Dairy Industrial Processing. ACS Appl. Mater. Interfaces 9, 26565–26573. https://doi.org/10.1021/acsami.7b06709